AGU PUBLICATIONS

JGR

Journal of Geophysical Research: Biogeosciences

RESEARCH ARTICLE
10.1002/2016JG003460

Key Points:
- Regional differences in $\delta^{13}C$ and $\delta^{18}O$ from earlywood and latewood were observed, which reflect a gradient in seasonal monsoon development
- Tree WUE inferred from latewood $\delta^{13}C$ exhibited greater sensitivity to moisture variation near the north limit of the monsoon system
- Summer air humidity has a significant latitudinal influence on the relative $\delta^{13}C$ and $\delta^{18}O$ values in cellulose of earlywood and latewood

Supporting Information:
- Supporting Information S1

Correspondence to:
P. Szejner,
paulszejner@email.arizona.edu

Citation:
Szejner, P., W. E. Wright, F. Babst, S. Belmecheri, V. Trouet, S. W. Leavitt, J. R. Ehleringer, and R. K. Monson (2016), Latitudinal gradients in tree ring stable carbon and oxygen isotopes reveal differential climate influences of the North American Monsoon System, *J. Geophys. Res. Biogeosci.*, *121*, doi:10.1002/2016JG003460.

Received 19 APR 2016
Accepted 10 JUL 2016
Accepted article online 18 JUL 2016

Latitudinal gradients in tree ring stable carbon and oxygen isotopes reveal differential climate influences of the North American Monsoon System

Paul Szejner[1,2], William E. Wright[1], Flurin Babst[1,3,4], Soumaya Belmecheri[1], Valerie Trouet[1], Steven W. Leavitt[1], James R. Ehleringer[5], and Russell K. Monson[1,6]

[1]Laboratory of Tree-Ring Research, University of Arizona, Tucson, Arizona, USA, [2]School of Natural Resources and the Environment, University of Arizona, Tucson, Arizona, USA, [3]Dendroclimatology Group, Swiss Federal Research Institute WSL, Birmensdorf, Switzerland, [4]W. Szafer Institute of Botany, Polish Academy of Sciences, Krakow, Poland, [5]Stable Isotope Ratio Facility for Environmental Research, Department of Biology, University of Utah, Salt Lake City, Utah, USA, [6]Department of Ecology and Evolutionary Biology, University of Arizona, Tucson, Arizona, USA

Abstract The arrival of the North American Monsoon System (NAMS) terminates a presummer hyperarid period in the southwestern United States (U.S.), providing summer moisture that is favorable for forest growth. Montane forests in this region rely on winter snowpack to drive much of their growth; the extent to which they use NAMS moisture is uncertain. We addressed this by studying stable carbon and oxygen isotopes in earlywood and latewood from 11 sites along a latitudinal gradient extending from Arizona and New Mexico to Utah. This study provides the first regional perspective on the relative roles of winter versus summer precipitation as an ecophysiological resource. Here we present evidence that Ponderosa pine uses NAMS moisture differentially across this gradient. $^{13}C/^{12}C$ ratios suggest that photosynthetic water use efficiency during latewood formation is more sensitive to summer precipitation at the northern than at the southern sites. This is likely due to the fact that NAMS moisture provides sufficiently favorable conditions for tree photosynthesis and growth during most years in the southern sites, whereas the northern sites experience larger summer moisture variability, which in some years is limiting growth. Cellulose $\delta^{18}O$ and $\delta^{13}C$ values revealed that photoassimilates in the southern sites were produced under higher vapor pressure deficit conditions during spring compared to summer, demonstrating a previously underappreciated effect of seasonal differences in atmospheric humidity on tree ring isotope ratios. Our findings suggest that future changes in NAMS will potentially alter productivity and photosynthetic water use dynamics differentially along latitudinal gradients in southwestern U.S. montane forests.

1. Introduction

Summer rainfall from the North American Monsoon System (NAMS) contributes to the bimodal precipitation pattern that defines the Sonoran Desert and Sky Island mountains, sustaining diverse ecosystems in northern Mexico and the southwestern United States (U.S.) [*Adams and Comrie*, 1997]. The NAMS is initiated in late spring following heating of the Sierra Madre Occidental and Mexican Plateau [*Douglas et al.*, 1993; *Higgins et al.*, 1997]. Continental heating in these regions creates a sea-land pressure gradient that facilitates the inland movement of low-altitude atmospheric moisture from the eastern tropical Pacific and Gulf of California with an additional source from the Gulf of Mexico in a high-altitude atmospheric circulation [*Higgins et al.*, 1997; *Wright et al.*, 2001; *Adams et al.*, 2014; *Metcalfe et al.*, 2015]. As the Northern Hemisphere summer develops, NAMS rainfall progresses northward in the form of frequent afternoon and evening convective storms.

Besides summer precipitation, winter precipitation is also an important resource for forests in the southwestern U.S. However, the amount of winter precipitation and its ecological influence decreases from the western boundary of the NAMS domain eastward—boundaries described during the 10th North American Monsoon Experiment, Science Working Group Meeting [*Castro et al.*, 2012; *Griffin et al.*, 2013]. Winter precipitation is not influenced by the higher-frequency processes that drive summer storms [*Nolin and Hall-McKim*, 2006] and is correlated instead with longer-term climate modes influenced by sea surface temperature in the Eastern Pacific Ocean [*Nolin and Hall-McKim*, 2006; *Vera et al.*, 2006]. Archeological evidence has revealed centennial-scale variation in the spatial domain of the NAMS, showing a more northerly occurrence of summer rain during the warmer conditions of the Medieval Climate Anomaly [*Coltrain and Leavitt*, 2002]. Continental

meteorological conditions can also influence the distribution and intensity of local NAMS precipitation. Wet conditions during summer, for example, can persist into early autumn, if the annually occurring Northern Hemisphere subtropical ridge is positioned to the north and northeast of the NAMS domain. In contrast, a southward shift of the subtropical ridge is linked to below-average precipitation, especially in the northern extent of the domain [*Higgins et al.*, 1997; *Castro et al.*, 2001].

Both summer and winter precipitation support montane forest ecosystems throughout the NAMS region. Different radial subdivisions of wood within an annual tree ring contain seasonal information on water use, thus enabling studies on the relative influence of seasonal precipitation on plant growth [*Meko and Baisan*, 2001; *Helle and Schleser*, 2004; *Stahle et al.*, 2009; *Griffin et al.*, 2013]. Many evergreen gymnosperms exhibit anatomical characteristics within annual rings that demarcate tissues with relatively large-diameter tracheids known as earlywood (EW) from adjacent tissues with dense, small-diameter tracheids, which are usually termed latewood (LW); LW usually ends with a sharp boundary adjacent to the following year's EW. Together, EW and LW from a single year form an annual tree ring in trees, where LW is present. In many trees from arid areas, a third wood anatomical characteristic can occasionally be identified, the so-called false ring or intra-annual density fluctuation (IADF), consisting of layers of tracheids with small diameters within the EW. IADFs are common in Ponderosa pine trees from strongly drought-limited sites in the southwestern U.S. Here IADFs can be distinguished from the actual LW in that they lack sharp terminal boundaries [*Babst et al.*, 2016]. These anatomical differences are the expression of cambium phenological processes related to temperature and water availability during incipient cellular division and subsequent formation and thickening of secondary cell walls [*Vaganov et al.*, 2006]. Trees and individual annual rings will exhibit different degrees of representation of these tissues, depending on the environmental conditions experienced during growth [*Meko and Baisan*, 2001; *Stahle et al.*, 2009; *Griffin et al.*, 2013].

Environmental and physiological mechanisms controlling carbon assimilation in trees can be measured not only by the relative growth of selected regions of annual rings but also by analyzing the stable isotope ratios (δ) of the wood cellulose [*Vaganov et al.*, 2009; *Leavitt*, 2010]. According to theory, the ratio between the intercellular CO_2 (c_i) concentration within leaves—controlled by the relative influences of stomatal conductance and carbon assimilation rate—and the atmospheric CO_2 concentration (c_a) can be interpreted as a proxy reflecting diffusive and metabolic isotope effects driving $^{13}CO_2$ discrimination [*Farquhar et al.*, 1982; *Ehleringer and Cerling*, 1995; *Roden and Ehleringer*, 2007]. The time-integrated c_i/c_a can accordingly be related to the $^{13}C/^{12}C$ ratio of photoassimilates and the plant tissues they compose, and this ratio is often expressed through measurements of cellulose $\delta^{13}C$. Examination of the cellulose $\delta^{13}C$ values in tree rings allows for physiological inferences about intrinsic photosynthetic water use efficiency (WUE) and climatic impacts [see, *Farquhar et al.*, 1982; *Francey and Farquhar*, 1982; *Leavitt et al.*, 2002; *Roden and Ehleringer*, 2007; *Gessler et al.*, 2014; *Treydte et al.*, 2014; *Frank et al.*, 2015].

Oxygen stable isotope ratios in wood cellulose are informative about water sources used by plants for growth and the atmospheric vapor pressure deficit (VPD) [*Roden et al.*, 2000]. Variation in the $^{18}O/^{16}O$ ratios of tree ring cellulose—expressed as $\delta^{18}O$ values—are often interpreted as reflecting interactions among source water $\delta^{18}O$, atmospheric VPD, and atmospheric water vapor $\delta^{18}O$. When interpreting tree ring $\delta^{18}O$ values, it is important to recognize mechanistic aspects, such as biochemical fractionation during sucrose synthesis and the proportion of photoassimilate oxygen that is exchanged with stem water at the site of wood cellulose synthesis [*Roden et al.*, 2000; *Gessler et al.*, 2014].

The annual bimodal winter-summer precipitation across the NAMS region, and the arid early-summer period that separates the two rainy seasons, provides opportunities to examine differential climate effects on the isotopic composition of tree ring tissues. In an effort to understand how montane forests in the NAMS geographic domain utilize water provided by seasonal precipitation modes, we undertook a regional study of annual tree rings in *Pinus ponderosa* (Douglas ex C. Lawson), one of the most common and locally dominant trees across the Western North America. We examined patterns of EW and LW production and stable isotope ratios of cellulose. We developed new observational approaches to understand the relative use of winter versus summer precipitation in forests along a south-to-north gradient of NAMS intensity. We hypothesize that the gradient of NAMS moisture leads to a latitudinal gradient in the degree to which forests utilize summer rain for their annual growth. Our main questions were as follows: (1) Can we identify regional and seasonal differences in $\delta^{13}C$ and $\delta^{18}O$ from the EW and LW portions of annual tree rings? (2) Can we detect a

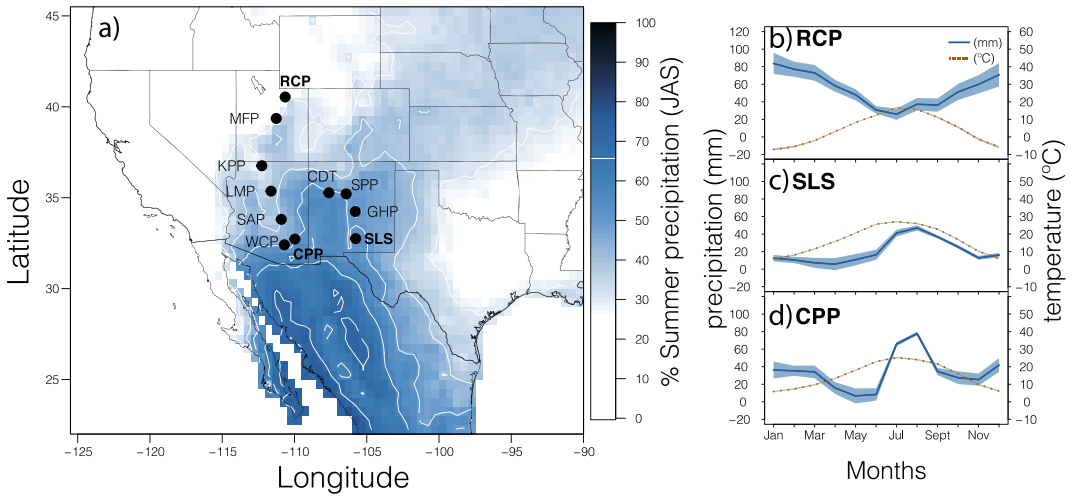

Figure 1. (a) Proportion (in %) of summer (July–September (JAS)) precipitation with respect to the total annual precipitation amount. Darker colors indicate higher summer precipitation proportion. The tree ring network in the U.S. extension of the NAMS is indicated with black dots. Climate diagrams of precipitation (pre) and temperature (tmp) for (b) northern (UT), (c) southeastern (NM), and (d) southwestern (AZ) regions of the NAMS.

physiological response by trees to variation in NAMS moisture through these isotopic ratios? (3) What are the spatiotemporal patterns in the physiological responses of Ponderosa pine trees, as differentially detected in EW and LW and inferred by $\delta^{13}C$ and $\delta^{18}O$, in the core and fringe regions of the NAMS domain? (4) Which climate variables best explain those spatiotemporal patterns?

2. Methods

2.1. Regional Characteristics

The climate of the U.S. extension of the NAMS region contains two general spatial gradients where winter precipitation decreases from northwest to southeast and summer precipitation decreases from south to north (Figure 1). At the northern limits of the region in Utah (UT), the precipitation regime is dominated by winter precipitation, with only 20–30% of precipitation occurring during the summer (Figure 1b). In the southeastern portion of the region in New Mexico (NM) average winter precipitation is less than the average summer precipitation total (Figure 1c). The reduction in total precipitation between Arizona (AZ) and NM is because moist air masses from the Pacific Ocean move eastward and progressively lose moisture [*Sheppard et al.*, 2002] In AZ and northern NM, a bimodal precipitation regime occurs with summer rainfall contributing 40–70% to the annual total (Figure 1d).

2.2. Data Collection

Forty-four α-cellulose stable isotope tree ring chronologies (1960–2012 C.E.) were developed from 11 sites within the NAMS region (Figure S1 in the supporting information). The 11 sites are distributed across the southwestern U.S. with five sites located in AZ, four sites in NM, and two sites in UT (Figure 1a). Four chronologies were developed at each site from EW and LW cellulose $\delta^{13}C$ and $\delta^{18}O$.

The sites and sampled trees were selected from montane forest ecosystems, which were dominated by *Pinus ponderosa*, and based on the following criteria: (1) excluding sites with large surrounding watersheds that could contribute runoff water to the observed site; (2) selecting medium-aged trees (e.g., 100–150 years); (3) selecting sites with evidence of low tree-to-tree canopy competition, and no evidence of past-century land use changes; (4) selecting trees that showed signs of vigorous recent growth with a well-formed and symmetrical crown; and (5) selecting trees with no or minimal occurrence of IADFs, which are indicative of a significant influence of the hyperarid period before the onset of summer rainfall [*Schulman*, 1938; *Wright et al.*, 2001; *Leavitt et al.*, 2002; *Babst et al.*, 2016]. The last criterion served our goal to study growth responses to winter and summer precipitation, rather than presummer drought. In order to secure enough wood material for the isotopic analysis at each site, we collected two to three cores from 20 to 30 trees using an increment borer of 5 mm diameter (inner cylinder).

Table 1. Site Characteristics and Statistics of Tree Ring Chronologies Used for Isotopic Analyses[a]

	Physical Characteristics					Tree Ring Chronology Statistics					
Site	Latitude (deg)	Longitude (deg)	Altitude (m above sea level)	Annual mean precip. (mm)	Annual mean temp. (°C)	Mean RWL (mm)	MS	*N*	Rbar	EPS	SNR
RCP	40.54	−110.64	2315	652	4.2	1.49	0.28	10	0.48	0.9	9.03
MFP	39.36	−111.26	2435	209	7.2	2.08	0.24	9	0.82	0.98	40.96
KPP	36.76	−112.26	2271	380	9.7	1.42	0.24	8	0.66	0.94	15.71
LMP	35.36	−111.62	2608	418	14.7	2.12	0.23	8	0.42	0.85	5.84
CDT	35.27	−107.62	2767	326	8.5	1.3	0.28	10	0.45	0.89	8.28
SPP	35.21	−106.42	2716	381	9.9	1.71	0.45	6	0.56	0.88	7.63
GHP	34.24	−105.79	2426	277	13.8	1.74	0.51	8	0.84	0.98	39.74
SAP	33.81	−110.91	2218	510	17.0	1.94	0.28	11	0.32	0.84	5.24
SLS	32.75	−105.77	2551	242	16.4	2.51	0.24	10	0.47	0.9	8.88
CPP	32.72	−109.97	2682	409	15.0	2.63	0.3	9	0.32	0.81	4.32
WCP	32.41	−110.7	2317	413	16.8	1.4	0.28	12	0.71	0.97	29.56

[a]Ring width length (RWL), mean sensitivity (MS), number of samples (*N*), mean correlation coefficient (Rbar), Expressed Population Signal (EPS), signal to noise ration (SNR).

2.2.1. Chronology Development and Dating

To ensure correct dating of the isotope measurements, samples were visually cross-dated following classic dendrochronological methods [*Stokes and Smiley*, 1996]. Briefly, samples were mounted using water-soluble hide glue, so that the samples to be analyzed for isotope composition could be unmounted easily and sectioned after dating. A tree ring chronology was developed for each site that included the 4–5 trees used for the isotopic analysis (Table 1). Each ring width series was detrended and standardized by fitting a 100 year cubic spline [*Cook and Peters*, 1997], followed by the calculation of a robust mean to compute the final ring width chronology (Table 1).

In order to assess patterns in the chronologies, we calculated several descriptive statistical metrics (Table 1). The mean sensitivity (MS) quantifies the interannual variation in growth between two adjacent rings, often interpreted as indicating the influence of climate on radial growth [*Bunn et al.*, 2013]; the signal-to-noise ratio (SNR) serves as an expression of the strength of the observed common signal among trees; the mean interseries correlation (Rbar) is the mean correlation coefficient resulting from comparing all possible segments of a predetermined length among all the series included in the chronology. In this study, a 50 year segment length and a 25 year lag between consecutive segments were used. The Expressed Population Signal (EPS) is based on the Rbar and has a possible range from 0 to 1 expressing the total signal present in the chronology. The EPS increases with sample size and number of samples, and values >0.85 indicates that the number of samples integrating the chronology is large enough to capture an adequate signal present in an infinitely replicated chronology [*Wigley et al.*, 1984].

2.2.2. Sample Preparation and Isotope Analysis

Each tree ring from 1960 to 2012 was sliced into three sections: the earlywood, which was split into two halves EW1(first half) and EW2 (second half) and the latewood (LW). Only EW1 and LW were used for isotopic analysis, with the EW2 subdivision being stored for future analysis. We assume that EW1 (hereafter referred to as "EW") is a proxy for winter and spring climate and LW is a proxy for summer climate. Each subdivision for each year was pooled from all trees per site into one combined sample, except every 10 years when we analyzed trees separately to quantify the intertree variability in isotopic composition (Figure S1).

Samples were ground to 20 mesh (0.84 mm) and pouched in permeable bags produced from a polymer fabric from Ankom technology. α-cellulose was extracted from each wood sample following a modification of the method described by *Leavitt and Danzer* [1993], with the addition of an NaOH extraction step. Lipid extraction was done with 2:1 toluene:ethanol solution in a Soxhlet apparatus for 24 h followed by 95% ethanol for 24 h. After rinsing, samples were boiled for 6 h, and then bleached in a solution of 7 g of sodium chlorite in 500 mL, adding glacial acetic acid to maintain a pH below 4, and then rinsed with deionized water. In the final step, samples were submersed in a 17% solution of sodium hydroxide for 60 min, rinsed with distilled water, bathed in a 10% acetic acid solution for 60 min, and then rinsed again. In order to obtain well-mixed (homogeneous) α-cellulose, fibers were separated by sonicating the material in 1 mL of chilled deionized water with 30 s of ultrasound by using a Hielscher UP200S ultrasonic probe [*Laumer et al.*, 2009].

The ratios of $^{13}C/^{12}C$ were measured for the CO_2 produced during α-cellulose combustion in a high-temperature conversion elemental analyzer coupled with a Thermo Delta Isotope Ratio Mass Spectrometer (TC/EA-IRMS) in the Environmental Isotope Laboratory of the Department of Geosciences at The University of Arizona. The $^{18}O/^{16}O$ ratios were measured on the CO produced by α-cellulose pyrolysis [*Saurer et al.*, 1998] in a TC/EA-IRMS at the Stable Isotope Ratio Facility for Environmental Research from the University of Utah. Isotopic values are expressed in the delta (δ) notation relative to the $\delta^{13}C$ Vienna Peedee belemnite ‰ and $\delta^{18}O$ Vienna SMOW ‰. The $\delta^{13}C$ sample accuracy was ±0.06‰ (standard deviation calculated from the average difference between measured internal standards, $n = 230$), and the $\delta^{18}O$ sample accuracy was ±0.24‰ ($n = 429$).

2.3. Data Analysis

Each $\delta^{13}C$ chronology was corrected for the ^{13}C "Suess effect" introduced by long-term trends in the stable carbon isotopic composition of atmospheric CO_2. Chronologies were also corrected for declines in $\delta^{13}C$ [*Suess*, 1955; *Field et al.*, 1995; *Francey et al.*, 1999; *McCarroll et al.*, 2009] that may result from a physiological response to rising CO_2 (the so-called PIN correction [see *Gagen et al.*, 2007]). To compare the EW and the LW $\delta^{13}C$, we estimated the mean annual difference between both sections and tested the statistical significance of differences using a *t* test and a Kolmogorov and Smirnov distribution test (Table S1 in the supporting information).

2.3.1. Seasonal Climate Response

To test tree response to climate variability, the isotope chronologies were compared with monthly and seasonal precipitation and temperature data from CRU TS3.21 [*Harris et al.*, 2014] and VPD at 700 hPa and 850 hPa computed using the Clausius-Clapeyron equation with air temperature and relative humidity obtained from the National Center for Environmental Prediction and National Center for Atmospheric Research [*Kistler et al.*, 2001]. The $\delta^{13}C$ and $\delta^{18}O$ chronologies were regressed against monthly climate records from the previous September through the following-year November of each growth year (13 month window). The EW chronologies from each site were compared with winter-spring (March–May) climate, and the LW chronologies were compared with winter-spring (March–May), and summer (June–August) climate.

The common signal among the sites was assessed with a principal component analysis (PCA) based on a covariance matrix, using the PCA function in the software package "R" {FactoMineR library}. Using the $\delta^{13}C$ and $\delta^{18}O$ values in EW and LW chronologies, six different PCAs were resolved in two different modes to show significant associations among sites. "Mode 1" corresponds to a biannual time series (i.e., EW_t, LW_t, EW_{t+1}, LW_{t+1}…EW_{t+n}, LW_{t+n}). "Mode 2" corresponds to the annual $\delta^{13}C$ and $\delta^{18}O$ for both EW and LW as separated variables and was correlated with geographically gridded monthly VPD.

3. Results

3.1. Regional Differences Between EW and LW $\delta^{13}C$ and $\delta^{18}O$

The $\delta^{18}O$ values of EW were significantly different (at $P < 0.05$) from LW for eight of the 11 study sites; the exceptions were the northern sites in UT (RCP and MFP) and one site in northern NM (SPP) (Figure 2) (Table S1). Similarly, the $\delta^{13}C$ values for EW and LW were significantly different at most sites, except the northern sites RCP, KPP, CDT, SPP, and SAP. A south-to-north gradient was observed in the difference between EW and LW with regard to mean $\delta^{13}C$ and $\delta^{18}O$. Interestingly, the LW $\delta^{13}C$ and $\delta^{18}O$ values at the southern sites were isotopically lighter (i.e., depleted in the heavier isotopes) compared to the EW, whereas at the northern sites, LW $\delta^{13}C$ and $\delta^{18}O$ values were similar or isotopically heavier (i.e., enriched in the heavier isotopes) than EW (Figure 2).

3.2. Monthly Climate Response

Considering all sites combined, the $\delta^{13}C$ and $\delta^{18}O$ values were negatively correlated with monthly mean precipitation and positively correlated with monthly mean VPD (Figure 3). In other words, the $\delta^{13}C$ and $\delta^{18}O$ values were isotopically heavier when precipitation was below average, and when mean monthly VPD was above average, during the growing period. EW $\delta^{13}C$ and $\delta^{18}O$ values were significantly correlated with winter and spring precipitation, and LW $\delta^{13}C$ and $\delta^{18}O$ values were significantly correlated with summer precipitation (Figures 3a and 3b). EW $\delta^{18}O$ values were significantly correlated with mean spring VPD, and LW $\delta^{18}O$ values were significantly correlated with mean summer VPD (Figures 3c and 3d). The significantly positive correlations between $\delta^{13}C$ with precipitation and VPD only differentiated the EW from LW in the summer months (Figures 3a and 3c).

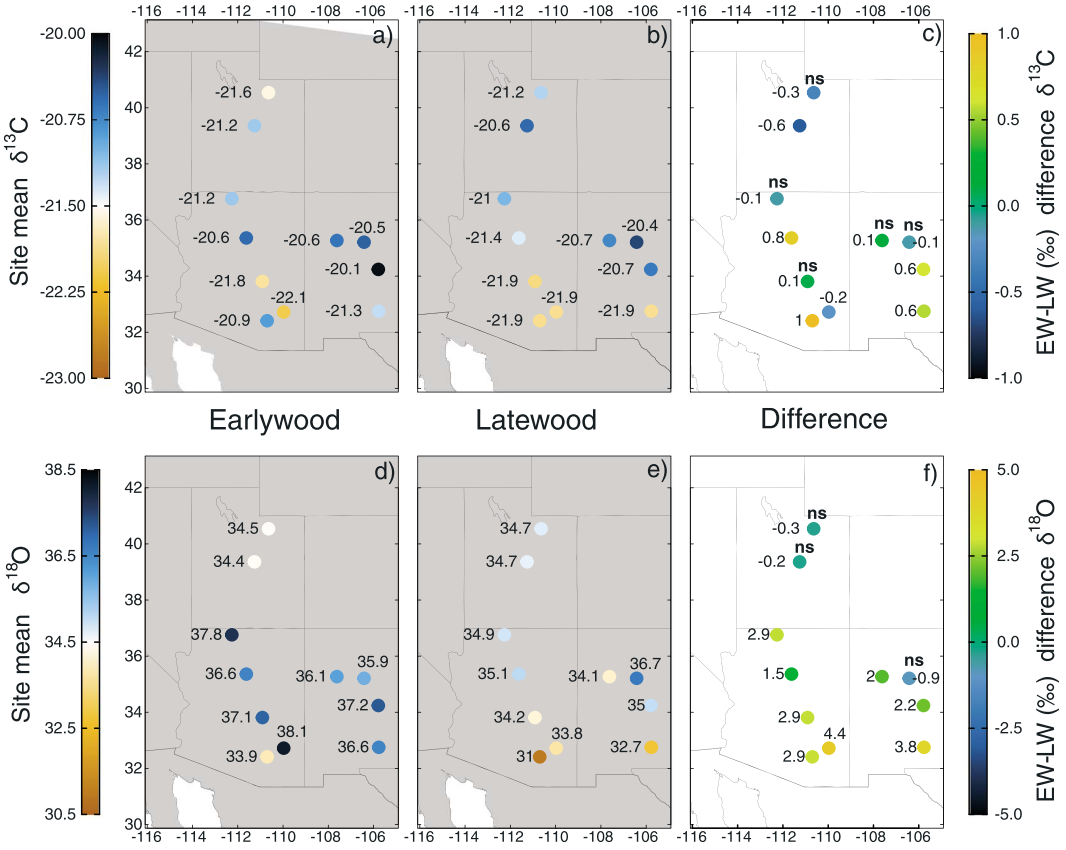

Figure 2. (top row) Regional δ^{13}C and (bottom row) δ^{18}O mean values (‰) and mean annual difference between EW and LW (‰). (a and d) EW, (b and e) LW, and (c and f) the mean annual difference between EW and LW. ns indicates no statistical difference at $P < 0.01$, based on a t test (Table S1).

Values of δ^{13}C in EW and LW reflect physiological responses to moisture variability, and this sensitivity is significant in the northern AZ, NM, and UT sites. There is a distinct south-to-north gradient in the degree to which LW δ^{13}C reflects summer precipitation amounts, with the correlations between LW δ^{13}C and mean summer precipitation at sites located in southern AZ not statistically significant (Figure 4). In contrast, sites located in northern Utah showed highly significant correlations between LW δ^{13}C and mean summer precipitation.

EW and LW δ^{18}O chronologies showed less variability in their sensitivity to spring or summer climate among sites compared to δ^{13}C chronologies (Figure 5). The EW δ^{18}O time series showed significant correlations with spring precipitation, VPD, and temperature variability at seven sites, whereas correlations between the LW chronologies and summer climate variables were significant only at the southern AZ and NM sites.

3.3. Regional Signal of EW_t and LW_t: Mode 1

The first principal component (PC1) of δ^{13}C from Mode 1 (combined EW and LW; see section 2) explained 42% of common variance across sites (Figure 6). The δ^{13}C PC1 time series showed two main features: decadal variability and an increasing trend over the last 30 years. The δ^{18}O PC1 from Mode 1 explained 45% of common variance, although the northern sites (RCP, MFP, and SPP) are not represented by this PC (Figure 6). The δ^{18}O PC1 also showed two main patterns: the intra-annual variability reflecting the winter and summer seasonality observed in EW and LW values and the low frequency variation of 10–20 years (Figure 6).

3.4. Regional Response Principal Component: Mode 2

Similar to Mode 1, PC1 of Mode 2 (EW and LW analyzed separately; see section 2) explained 50% of the variance in the EW δ^{13}C across sites and 45% of the variance of the LW δ^{13}C (Figure 7). PC1 of Mode 2 from EW δ^{18}O and LW δ^{18}O explained 34% and 25% of the total variance, respectively. Pearson correlation coefficients

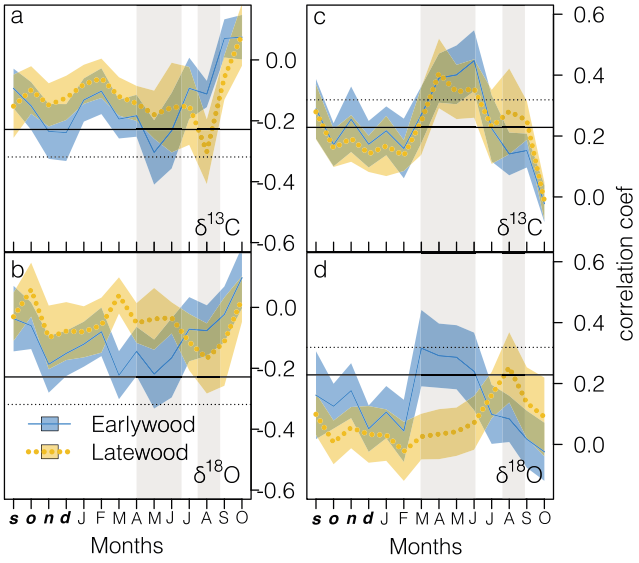

Figure 3. Mean and 95% confidence intervals across all study sites of monthly Pearson correlation coefficients of EW (blue) and LW (orange) with (a and b) precipitation and (c and d) VPD at 700 hPa. The grey shading indicates the coherent seasons with significant correlations. The horizontal continuous and dashed lines mark the significance levels for Pearson correlations at $\alpha = 0.05$ and $\alpha = 0.01$, respectively. The bold-italic letters mark the months from previous year on the *x* axis.

between PC1 Mode 2 scores and the gridded mean seasonal VPD showed a significant seasonal influence of atmospheric water demand on both isotopes across the NAMS region (see also monthly field correlation analysis in the Figure 3). Additionally, the common pattern in the $\delta^{13}C$ network showed a significant correlation coefficient between EW and LW ($r = 0.84$). The $\delta^{18}O$ common signal showed a distinct difference between spring and summer influences in the southernmost portion of the study domain.

4. Discussion

The spatial pattern of subannual tree ring $\delta^{13}C$ and $\delta^{18}O$ time series from 1960 to 2012 C.E. allowed us to identify differences between winter versus summer precipitation influences on Ponderosa pine tree growth across the arid U.S. Southwest. The seasonality of the climate varied markedly from south-to-north across the U.S. extension of the NAMS. In the southern portion of the domain (AZ), a bimodal precipitation pattern is clearly evident with both winter and summer rainfall providing significant fractions of total annual rainfall. The west-to-east difference between the Southern AZ and the Southern NM sites points toward a possible effect of the total amounts of moisture delivered between seasons. However, the low number of sites prevents us from resolving the precipitation longitudinal effect. In the northern portion of the domain, the proportion of winter precipitation is greater, with a varying contribution of summer monsoon rain (Figure 4) [*Higgins et al.*, 1997; *Castro et al.*, 2001; *Dominguez et al.*, 2008]. At the northernmost site, in the Uinta Mountains near Salt Lake City, UT, summer monsoon activity consists of weak, infrequent surges of moisture that break away from the northern boundary of the monsoon circulation. In fact, at the most northern sites (RCP and MFP), the percentage of summer rainfall associated with the timing of monsoon circulation is as low as 10% (Figure 1).

The $\delta^{13}C$ and $\delta^{18}O$ values of EW and LW revealed geospatial patterns that reflect the decreasing south-to-north gradient of summer precipitation (Figure 2). The mean correlation between $\delta^{13}C$ and $\delta^{18}O$ in EW with monthly precipitation was significant ($P < 0.05$) only for winter and spring precipitation across the entire gradient, whereas the correlations between $\delta^{13}C$ and $\delta^{18}O$ in LW with monthly precipitation were significant for summer precipitation (Figures 3a and 3b). These results confirm previous observations in which LW formation was attributed to the growth period associated with delivery of NAMS moisture [*Meko and Baisan*, 2001; *Therrell et al.*, 2002; *Stahle et al.*, 2009; *Griffin et al.*, 2011]. Our results extend these past observations to a new set of 11 sites and provide much needed insight into relations between tree ring isotope ratios and the seasonality of precipitation at the northern fringe of the NAMS domain. Consistent with past studies of tree ring stable isotopes [e.g., *Leavitt et al.*, 2002, 2011], our study also showed photosynthetic water use efficiency in LW to be negatively correlated with summer precipitation, and in correlations of $\delta^{13}C$ and $\delta^{18}O$ against mean monthly precipitation our studies revealed that the heaviest isotope values were correlated with the driest conditions and the lightest isotope values were correlated with the wettest conditions, as predicted by mechanistic models [*Gessler et al.*, 2014].

The relative enrichment of EW cellulose in ^{18}O and ^{13}C isotopes, compared to LW cellulose, which we observed in the southernmost sites, indicates that photoassimilates were produced under higher VPD conditions during the spring snowmelt period compared to summer. Our data are the first to provide evidence that seasonal

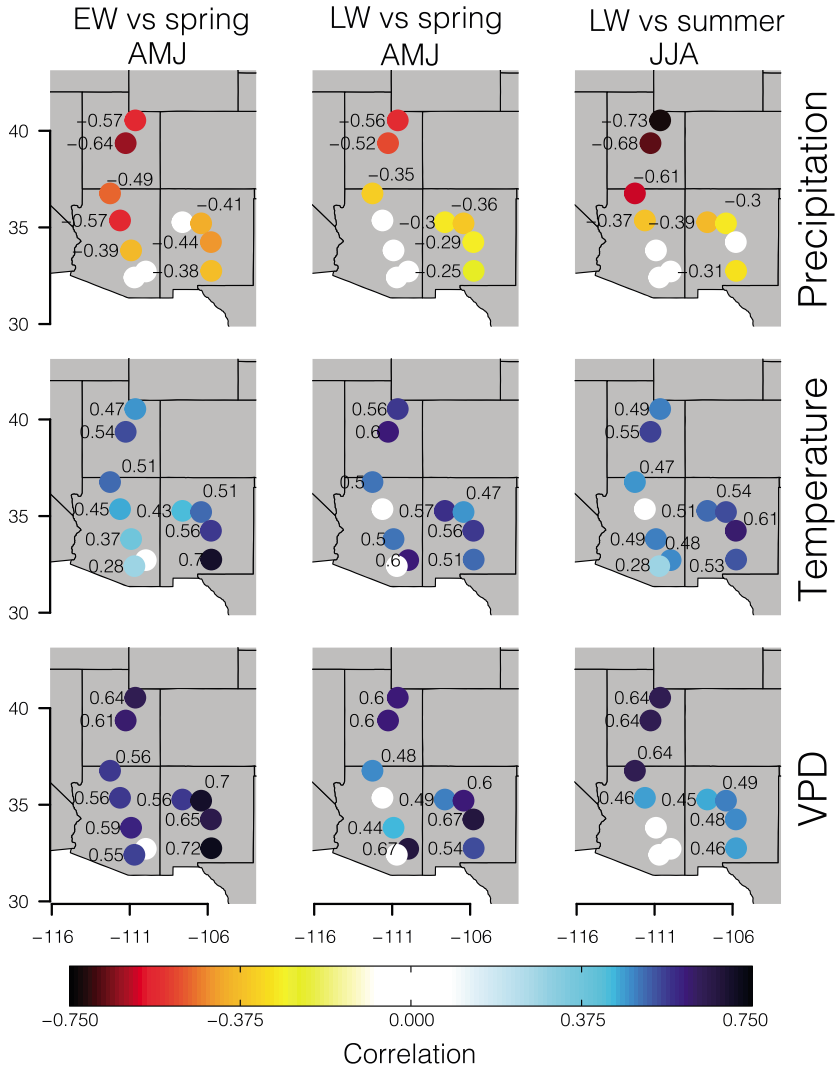

Figure 4. Site-specific Pearson correlation coefficients between (top row) δ^{13}C chronologies and precipitation, (middle row) temperature, and (bottom row) VPD 700 hPa from 1960 to 2012 C.E. Correlation coefficients were calculated between (left column) δ^{13}C EW and (middle column) LW and spring (AMJ) precipitation, temperature, and VPD. (right column) In addition to this, correlation coefficients were calculated between δ^{13}C LW and summer (JJA) climate variables. Statistically nonsignificant correlations are shown in white.

differences in VPD drive divergent patterns in the δ^{13}C and δ^{18}O values of EW versus LW along the latitudinal gradient (Figure 2). The influence of seasonal atmospheric VPD dynamics was more pronounced for δ^{18}O, compared to δ^{13}C, emphasizing different seasonal influences of atmospheric water demand on leaf water isotopic fractionation. The fact that we observed significant positive correlations between EW δ^{18}O and monthly VPD in spring, as well as between LW δ^{18}O and monthly VPD in midsummer and fall, and no significant correlation between LW δ^{18}O and monthly VPD in spring, suggests that there is no persistent memory effect imprinted in the oxygen isotopes from spring to summer [*Helle and Schleser*, 2004; *Kagawa et al.*, 2006]. The positive correlations with VPD reflect the heavier ^{18}O/^{16}O isotope signal of leaf water during greater evaporative enrichment in periods with low atmospheric humidity [*Roden and Ehleringer*, 2007]. These results suggest the existence of a previously underappreciated effect of the extreme differences of atmospheric humidity between spring and summer, which can lead to significant differences in the isotopic values in tree rings along this latitudinal transect. The summer arrival of the NAMS creates a relatively humid break in the otherwise hot, hyperarid climate of early summer in the U.S. Southwest and apparently allows higher-elevation forests to efficiently utilize warm-season precipitation for photosynthetic carbon assimilation during the late-growing season.

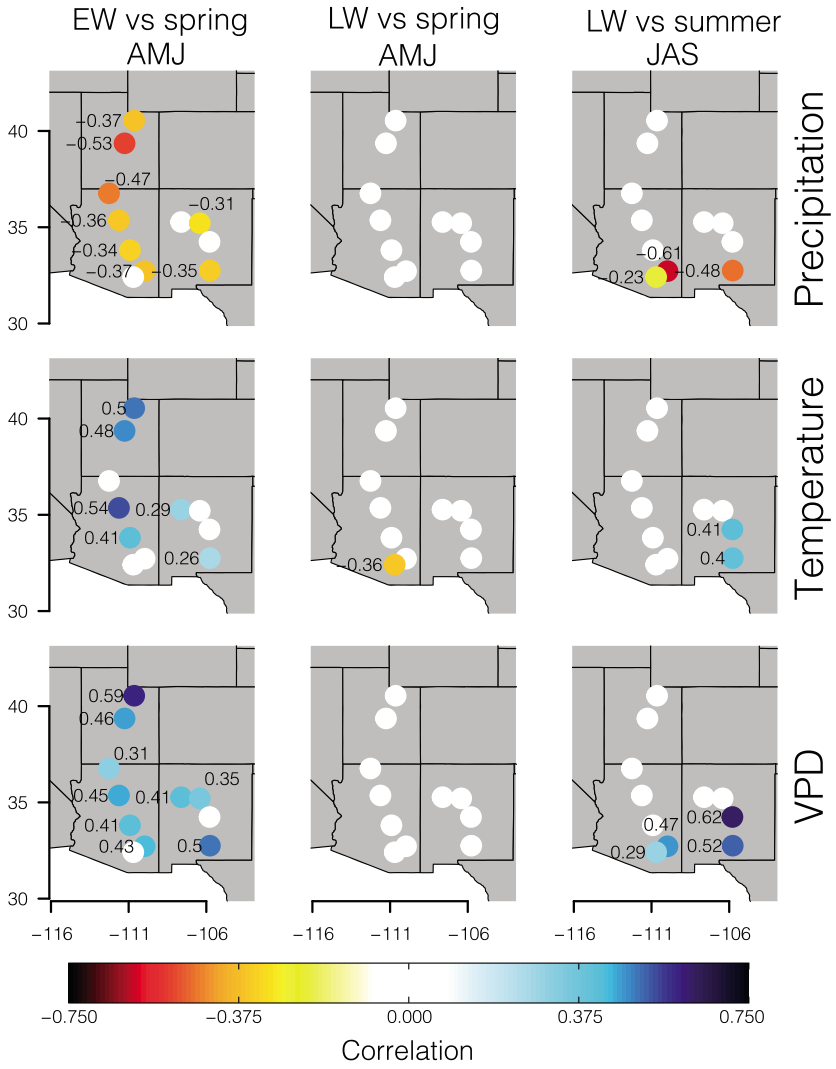

Figure 5. Site-specific Pearson correlation coefficients between (top row) δ^{18}O chronologies and precipitation, (middle row) temperature and (bottom row) VPD at 700 hPa from 1960 to 2012 C.E. Correlation coefficients were calculated between (left column) δ^{18}O EW and (middle column) LW and spring (AMJ) precipitation, temperature, and VPD, and (right column) between δ^{18}O LW and summer (JAS) climate variables. Statistically nonsignificant correlations are shown in white.

However, further research must be conducted in order to completely disentangle the relative influences of tree source water and evaporative enrichment on tree ring cellulose isotope values.

The significant negative correlations between the δ^{13}C of EW and late-winter to spring precipitation were similar across all sites (Figure 4). The δ^{13}C of LW samples, however, showed strong latitudinal differences when correlated with interannual variation in summer precipitation and VPD, with higher correlations emerging for the northern sites. These correlations indicate that at the northern sites, photosynthetic WUE responded strongly to interannual dynamics in mean summer precipitation and VPD, whereas no such effect occurred at the southern sites in AZ. The southern sites are located in that part of the U.S. extension of the NAMS that receives the highest fractions and amounts of summer moisture compared to northern and eastern sites (Figure 1). Accordingly, the nonsignificant relationships between δ^{13}C of LW and mean precipitation and VPD at the southern sites in AZ and the lower values in the δ^{13}C could suggest that summer monsoon moisture during most years provides sufficiently favorable conditions for tree photosynthesis and growth. In the northern sites, interannual variation in NAMS precipitation is likely to be more variable, providing sufficient moisture to drive LW production during some years. We note, however, that LW production in the northern sites might utilize stored carbon that was assimilated the previous spring, especially during years with lesser amounts of summer

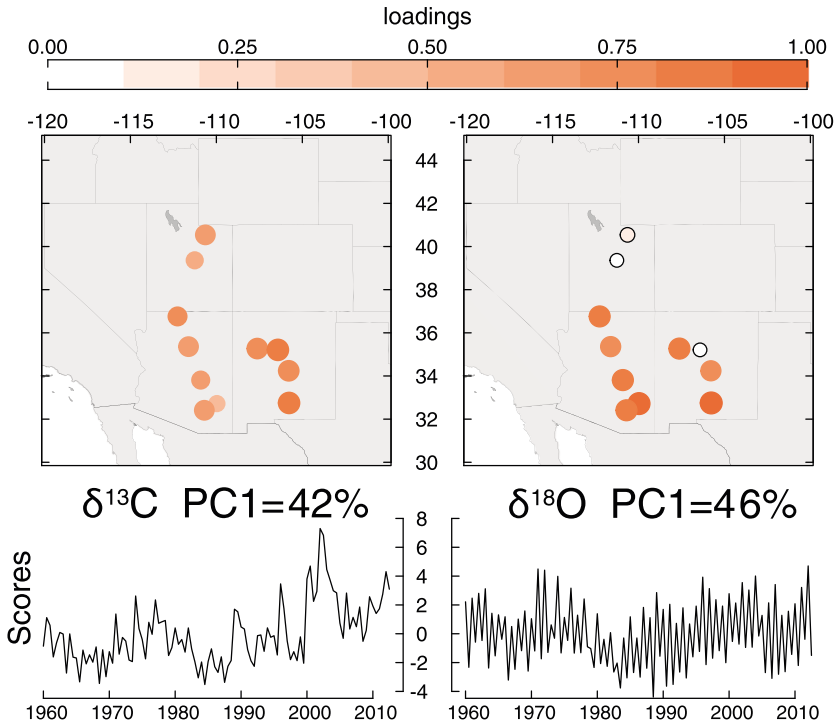

Figure 6. First principal components (PC1) of δ^{13}C and δ^{13}O time series in Mode 1 (combined EW and LW; see section 2) expressing the common seasonal variability across sites. (top row) The loadings of individual sites on PC1 and (bottom row) the corresponding PC1 time series are shown.

precipitation. This could bias LW isotope values toward those of the colder, drier spring period in years with limited summer moisture. More research will be needed to quantify the relative importance of stored versus recently acquired photoassimilates (i.e., the importance of "the memory effect" [*Ogle et al.*, 2015]).

The latitudinal differentiation among sites was also observed in δ^{18}O in LW (Figure 5). The southern AZ and NM sites were the only sites showing evidence of negative correlations between LW δ^{18}O and summer precipitation—i.e., greater enrichment in the ^{18}O composition of cellulose produced during periods with less summer precipitation. This pattern has been previously observed in regard to weaker monsoon activity [*Wright et al.*, 2001; *Roden and Ehleringer*, 2007]. These results indicate that the biophysical processes of leaf water exchange are indeed sensitive to interannual variations in summer precipitation at these southern sites, but as revealed in the LW δ^{13}C, that the physiological control over photosynthetic WUE is not strong.

The strongest correlations between δ^{18}O in LW and summer VPD were observed for trees in the central and southern mountains of NM. This positive relationship indicated that during dry periods with weaker monsoon activity and lower atmospheric humidity, ^{18}O evaporative enrichment of leaf water was greater. The presence of these significant correlations between LW δ^{18}O and variance in summer moisture in the southern sites, but not the northern sites, further supports the importance of summer monsoon moisture on biophysical processes in the southernmost NAMS regions.

The principal component analysis provided insight in time-dependent oscillations in the influence of seasonal climate on the δ^{13}C and δ^{18}O ratios of tree ring cellulose. The common signal for δ^{13}C and δ^{18}O in EW and LW revealed a positive trend over the past three decades, suggesting time-dependent greater intrinsic photosynthetic WUE at all sites [*Bert et al.*, 1997; *Maseyk et al.*, 2011; *Peñuelas et al.*, 2011; *Saurer et al.*, 2014; *Frank et al.*, 2015] during an exceptionally hot and dry decade in the southwestern U.S. This period included the extreme drought of 2002–2003 as it is observed in our δ^{13}C records (Figures 6 and 7), which has been identified as the most extreme drought observed in the southwestern U.S. for at least the last seven decades [*Breshears et al.*, 2005]. The δ^{18}O common signal shows the same low frequency, with a positive trend in the EW for the last three decades (Figures 6 and 7), indicating that water limitations on tree functioning have indeed been significant.

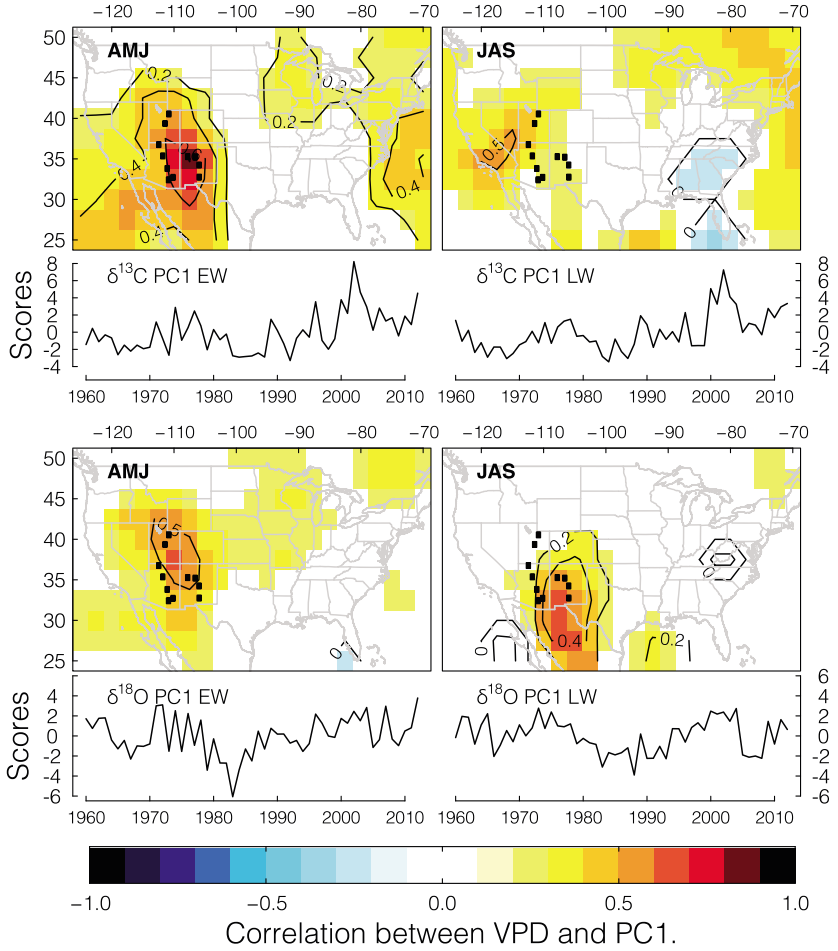

Figure 7. Field correlations of the first component (PC1) from Mode 2 derived from the δ^{18}O and δ^{13}C EW and LW chronologies, loaded independently (see section 2). Each colored pixel in the maps corresponds to the correlation coefficient between (left column) the spring (AMJ) mean VPD at 850 hPa record 1960–2012 and the PC1 EW (left maps) and (right column) summer (JAS) mean VPD record 1960–2012 and the PC1 LW. Noncolored pixels correspond to nonsignificant correlation at $\alpha = 0.05$ significance level. (Figures S4–S12).

However, the δ^{18}O observations also clearly showed a stationary seasonal shift from EW to LW, which supports our observation about the site-specific seasonal difference between winter and summer moisture sources.

Climate projections in the NAMS region predict a slight decrease in winter precipitation over out study region and no change in the total amount of summer-monsoon precipitation, although monthly projections predict a slight decrease in monsoon precipitation through July and a slight increase in September and October over our study region [*Cook and Seager*, 2013]. These projections suggest a longer hyperarid period with a later monsoon onset in the NAMS core region. Additional climate projections predict a temperature-driven increase in the warm-season VPD in the southwestern U.S. [*Williams et al.*, 2013]. Collectively, our results and the climate projections for the NAMS region foreshadow increased forest stress [*McDowell et al.*, 2015]. The physiological effects under the environmental conditions indicated by these projections will certainly be controlling carbon assimilation and water transpiration. However, the effects of water availability and VPD are dynamically related and mixed in to the isotopic signal of the cellulose, and further efforts must be made to decouple these environmental effects using carbon and oxygen isotopes in tree rings.

5. Conclusions

This study identified two main regional and seasonal differences in δ^{13}C and δ^{18}O from subannual tree ring records on trees in the NAMS region. First, δ^{13}C in LW was sensitive to interannual summer moisture

variability at the northern sites, with diminishing sensitivity toward the southern sites. Second, the seasonal (EW-LW) difference in $\delta^{18}O$ was significant in the southern sites, whereas no difference was observed at the northern sites. These observations reveal that trees of Ponderosa pine have differential access to warm season precipitation along the south-to-north track of the NAMS and that the differential access to summer rain influences the efficiency with which trees use limited soil moisture to support annual productivity.

There was coherence in the cross-site variations in stable isotope values from this network supporting a robust regional and seasonal climatic signal. The spatial relationships with VPD, temperature, and precipitation provided supporting evidence that $\delta^{13}C$ and $\delta^{18}O$ values are useful to infer seasonal moisture availability in semiarid to arid environments [*Roden and Ehleringer*, 2007; *Leavitt et al.*, 2011]. These findings are relevant with respect to the future vigor of Ponderosa pine-dominated mountain forests in the southwestern U.S. because moisture sources from two different seasons (i.e., snowpack and monsoon rainfall) likely have different competitive advantages for mountain forests that depend only on one source of water. Furthermore, acknowledging that winter and summer precipitation are independent of each other, we expect in the NAMS region, stronger hyperarid periods before monsoon onset, and increasing evaporative demand, especially during the drier periods, in the face of ongoing anthropogenic climate change. The possibility to derive seasonal moisture variability from subannual tree ring records carries great potential to model paleoclimatic dynamics in the NAMS region during the Medieval climate anomaly [*Stahle et al.*, 2009; *Leavitt et al.*, 2011; *Griffin et al.*, 2013]. This anomalously warm paleo-period is a potential analog to future climate change projections, and we may be able to use insight from tree rings to infer valuable information on possible future impacts on ecosystem functioning and its societal implications.

Acknowledgments
This study was supported by a grant from the Macrosystems program in the Emerging Frontiers section of the U.S. National Science Foundation (NSF award 1065790), and the Interuniversity Training Program in Continental-scale Ecology (NSF award 1137336). F.B. acknowledges funding from the Swiss National Science Foundation (grant P300P2_154543). We thank Leon Prescott Wells, Monica Vogel, Megan Mckey, Grace Kim, Alyssa Langford Abbey, and Seth Stephens for excellent technical assistance. The Tree ring data and isotope chronologies will be archived in the International Tree-Ring Databank or will be made available upon request to Paul Szejner (paulszejner@email.arizona.edu).

References

Adams, D. K., and A. C. Comrie (1997), The North American monsoon, *Bull. Am. Meteorol. Soc.*, *78*(10), 2197–2213, doi:10.1175/1520-0477(1997)078<2197:TNAM>2.0.CO;2.

Adams, D. K., C. Minjarez, Y. Serra, A. Quintanar, L. Alatorre, A. Granados, E. Vázquez, and J. Braun (2014), Mexican GPS tracks convection from North American Monsoon, *Eos Trans. AGU*, *95*(7), 61–62, doi:10.1002/2014EO070001.

Babst, F., W. E. Wright, P. Szejner, L. Wells, S. Belmecheri, and R. K. Monson (2016), Blue intensity parameters derived from Ponderosa pine tree rings characterize intra-annual density fluctuations and reveal seasonally divergent water limitations, *Trees*, doi:10.1007/s00468-016-1377-6.

Bert, D., S. W. Leavitt, and J.-L. Dupouey (1997), Variationa of wood δ13C and water-use efficiency of Abies alba duringthe last century, *Ecology*, *78*(5), 1588–1596, doi:10.1890/0012-9658(1997)078[1588:VOWCAW]2.0.CO;2.

Breshears, D. D., et al. (2005), Regional vegetation die-off in response to global-change-type drought, *Proc. Natl. Acad. Sci. U.S.A.*, *102*(42), 15,144–15,148, doi:10.1073/pnas.0505734102.

Bunn, A. G., E. Jansma, M. Korpela, R. D. Westfall, and J. Baldwin (2013), Using simulations and data to evaluate mean sensitivity (ζ) as a useful statistic in dendrochronology, *Dendrochronologia*, *31*(3), 250–254, doi:10.1016/j.dendro.2013.01.004.

Castro, C. L., T. B. McKee, and R. A. Pielke (2001), The relationship of the North American Monsoon to tropical and North Pacific sea surface temperatures as revealed by observational analyses, *J. Clim.*, *14*(24), 4449–4473, doi:10.1175/1520-0442(2001)014<4449:TROTNA>2.0.CO;2.

Castro, C. L., H.-I. Chang, F. Dominguez, C. Carrillo, J.-K. Schemm, and H.-M. H. Juang (2012), Can a regional climate model improve the ability to forecast the North American Monsoon?, *J. Clim.*, *25*, 8212–8237, doi:10.1175/JCLI-D-11-00441.1.

Coltrain, J. B., and S. W. Leavitt (2002), Climate and diet in Fremont prehistory: Economic variability and abandonment of maize agriculture in the Great Salt Lake basin, *Am. Antiq.*, *67*(3), 453, doi:10.2307/1593822.

Cook, B. I., and R. Seager (2013), The response of the North American Monsoon to increased greenhouse gas forcing, *J. Geophys. Res. Atmos.*, *118*, 1690–1699, doi:10.1002/jgrd.50111.

Cook, E. R., and K. Peters (1997), Calculating unbiased tree-ring indices for the study of climatic and environmental change, *Holocene*, *7*(3), 361–370, doi:10.1177/095968369700700314.

Dominguez, F., P. Kumar, and E. R. Vivoni (2008), Precipitation recycling variability and ecoclimatological stability—A study using NARR data. Part II: North American monsoon region, *J. Clim.*, *21*(20), 5187–5203, doi:10.1175/2008JCLI1760.1.

Douglas, M. W., R. A. Maddox, K. Howard, and S. Reyes (1993), The Mexican monsoon, *J. Clim.*, *6*, 1665–1677, doi:10.1175/1520-0442(1993)006<1665:TMM>2.0.CO;2.

Ehleringer, J. R., and T. E. Cerling (1995), Atmospheric CO(2) and the ratio of intercellular to ambient CO(2) concentrations in plants, *Tree Physiol.*, *15*(2), 105–111, doi:10.1093/treephys/15.2.105.

Farquhar, G. D., M. H. Oleary, and J. A. Berry (1982), On the relationship between carbon isotope discrimination and the inter-cellular carbondionxide concentration in leaves, *Aust. J. Plant Physiol.*, *9*(2), 121–137.

Field, C. B., R. B. Jackson, and H. A. Mooney (1995), Stomatal responses to increased CO2: Implications from the plant to the global scale, *Plant Cell Environ.*, *18*, 1214–1225.

Francey, R., and G. Farquhar (1982), An explanation of 13C/12C variations in tree rings, *Nature*, *297*, 28–31.

Francey, R., C. Allison, and D. Etheridge (1999), A 1000-year high precision record of δ13C in atmospheric CO2, *Tellus, Ser. B*, *51*, 170–193.

Frank, D. C., et al. (2015), Water-use efficiency and transpiration across European forests during the Anthropocene, *Nat. Clim. Change*, *5*(6), 579–583, doi:10.1038/nclimate2614.

Gagen, M., D. McCarroll, N. J. Loader, I. Robertson, R. Jalkanen, and K. J. Anchukaitis (2007), Exorcising the 'segment length curse': Summer temperature reconstruction since AD 1640 using non-detrended stable carbon isotope ratios from pine trees in northern Finland, *Holocene*, *17*(4), 435–446, doi:10.1177/0959683607077012.

Gessler, A., J. P. Ferrio, R. Hommel, K. Treydte, R. A. Werner, and R. K. Monson (2014), Stable isotopes in tree rings: Towards a mechanistic understanding of isotope fractionation and mixing processes from the leaves to the wood, *Tree Physiol.*, *34*(8), 796–818, doi:10.1093/treephys/tpu040.

Griffin, D., D. M. Meko, R. Touchan, S. W. Leavitt, and C. A. Woodhouse (2011), Latewood chronology development for summer-moisture reconstruction in the US Southwest, *Tree-Ring Res.*, *67*(2), 87–101, doi:10.3959/2011-4.1.

Griffin, D., C. A. Woodhouse, D. M. Meko, D. W. Stahle, H. L. Faulstich, C. Carrillo, R. Touchan, C. L. Castro, and S. W. Leavitt (2013), North American monsoon precipitation reconstructed from tree-ring latewood, *Geophys. Res. Lett.*, *40*, 954–958, doi:10.1002/grl.50184.

Harris, I., P. D. Jones, T. J. Osborn, and D. H. Lister (2014), Updated high-resolution grids of monthly climatic observations - The CRU TS3.10 dataset, *Int. J. Climatol.*, *34*(3), 623–642, doi:10.1002/joc.3711.

Helle, G., and G. H. Schleser (2004), Beyond CO2-fixation by Rubisco - An interpretation of C-13/C-12 variations in tree rings from novel intra-seasonal studies on broad-leaf trees, *Plant Cell Environ.*, *27*(3), 367–380, doi:10.1111/j.0016-8025.2003.01159.x.

Higgins, R. W., Y. Yao, and X. L. Wang (1997), Influence of the North American Monsoon system on the U.S. summer precipitation regime, *J. Clim.*, *10*(10), 2600–2622, doi:10.1175/1520-0442(1997)010<2600:IOTNAM>2.0.CO;2.

Kagawa, A., A. Sugimoto, and T. C. Maximov (2006), 13CO2 pulse-labelling of photoassimilates reveals carbon allocation within and between tree rings, *Plant Cell Environ.*, *29*(8), 1571–1584, doi:10.1111/j.1365-3040.2006.01533.x.

Kistler, R., et al. (2001), The NCEP-NCAR 50-year reanalysis: Monthly means CD-ROM and documentation, *Bull. Am. Meteorol. Soc.*, *82*(2), 247–268.

Laumer, W., L. Andreu, G. Helle, G. H. Schleser, T. Wieloch, and H. Wissel (2009), A novel approach for the homogenization of cellulose to use micro-amounts for stable isotope analyses, *Rapid Commun. Mass Spectrom.*, *23*(13), 1934–1940, doi:10.1002/rcm.4105.

Leavitt, S. W. (2010), Tree-ring C-H-O isotope variability and sampling, *Sci. Total Environ.*, *408*(22), 5244–5253, doi:10.1016/j.scitotenv.2010.07.057.

Leavitt, S. W., and S. R. Danzer (1993), Method for batch processing small wood samples to holocellulose for stable-carbon isotope analysis, *Anal. Chem.*, *65*(1), 87–89, doi:10.1021/ac00049a017.

Leavitt, S. W., W. E. Wright, and A. Long (2002), Spatial expression of ENSO, drought, and summer monsoon in seasonal δ 13 C of ponderosa pine tree rings in southern Arizona and New Mexico, *J. Geophys. Res.*, *107*(D18), 4349, doi:10.1029/2001JD001312.

Leavitt, S. W., C. A. Woodhouse, C. L. Castro, W. E. Wright, D. M. Meko, R. Touchan, D. Griffin, and B. Ciancarelli (2011), The North American monsoon in the U.S. Southwest: Potential for investigation with tree-ring carbon isotopes, *Quat. Int.*, *235*(1-2), 101–107, doi:10.1016/j.quaint.2010.05.006.

Maseyk, K., D. Hemming, A. Angert, S. W. Leavitt, and D. Yakir (2011), Increase in water-use efficiency and underlying processes in pine forests across a precipitation gradient in the dry Mediterranean region over the past 30 years, *Oecologia*, *167*(2), 573–585, doi:10.1007/s00442-011-2010-4.

McCarroll, D., M. H. Gagen, N. J. Loader, I. Robertson, K. J. Anchukaitis, S. Los, G. H. F. Young, R. Jalkanen, A. Kirchhefer, and J. S. Waterhouse (2009), Correction of tree ring stable carbon isotope chronologies for changes in the carbon dioxide content of the atmosphere, *Geochim. Cosmochim. Acta*, *73*(6), 1539–1547, doi:10.1016/j.gca.2008.11.041.

McDowell, N. G., et al. (2015), Multi-scale predictions of massive conifer mortality due to chronic temperature rise, *Nat. Clim. Change*, doi:10.1038/nclimate2873, in press.

Meko, D. M., and C. H. Baisan (2001), Pilot study of latewood-width of conifers as an indicator of variability of summer rainfall in the North American monsoon region, *Int. J. Climatol.*, *21*(6), 697–708, doi:10.1002/joc.646.

Metcalfe, S. E., J. A. Barron, and S. J. Davies (2015), The Holocene history of the North American Monsoon: "Known knowns" and "known unknowns" in understanding its spatial and temporal complexity, *Quat. Sci. Rev.*, *120*, 1–27, doi:10.1016/j.quascirev.2015.04.004.

Nolin, A. W., and E. A. Hall-McKim (2006), Frequency modes of monsoon precipitation in Arizona and New Mexico, *Mon. Weather Rev.*, *134*(12), 3774–3781, doi:10.1175/MWR3244.1.

Ogle, K., J. J. Barber, G. A. Barron-Gafford, L. P. Bentley, J. M. Young, T. E. Huxman, M. E. Loik, and D. T. Tissue (2015), Quantifying ecological memory in plant and ecosystem processes, *Ecol. Lett.*, *18*(3), 221–235, doi:10.1111/ele.12399.

Peñuelas, J., J. G. Canadell, and R. Ogaya (2011), Increased water-use efficiency during the 20th century did not translate into enhanced tree growth, *Global Ecol. Biogeogr.*, *20*(4), 597–608, doi:10.1111/j.1466-8238.2010.00608.x.

Roden, J., and J. R. Ehleringer (2007), Summer precipitation influences the stable oxygen and carbon isotopic composition of tree-ring cellulose in Pinus ponderosa, *Tree Physiol.*, *27*(4), 491–501, doi:10.1093/treephys/27.4.491.

Roden, J., G. Lin, and J. R. Ehleringer (2000), A mechanistic model for interpretation of hydrogen and oxygen isotope ratios in tree-ring cellulose, *Geochim. Cosmochim. Acta*, *64*(1), 21–35, doi:10.1016/S0016-7037(99)00195-7.

Saurer, M., I. Robertson, R. Siegwolf, and M. Leuenberger (1998), Oxygen isotope analysis of cellulose: An interlaboratory comparison, *Anal. Chem.*, *70*(10), 2074–2080, doi:10.1021/ac971022f.

Saurer, M., et al. (2014), Spatial variability and temporal trends in water-use efficiency of European forests, *Global Change Biol.*, *20*, 3700–3712, doi:10.1111/gcb.12717.

Schulman, E. (1938), Classification of false annual rings in Monterey pine, *Tree-Ring Bull.*, *4*, 4–7.

Sheppard, P. R., A. C. Comrie, G. D. Packin, K. Angersbach, and M. K. Hughes (2002), The climate of the US Southest, *Clim. Res.*, *21*, 219–238.

Stahle, D. W., M. K. Cleaveland, H. D. Grissino-Mayer, R. D. Griffin, F. K. Fye, M. D. Therrell, D. J. Burnette, D. M. Meko, J. Villanueva-Diaz, and J. Villanueva Diaz (2009), Cool- and warm-season precipitation reconstructions over Western New Mexico, *J. Clim.*, *22*(13), 3729–3750, doi:10.1175/2008JCLI2752.1.

Stokes, M. A., and T. L. Smiley (1996), *An Introduction to Tree-Ring Dating*, The Univ. of Arizona Press, Tucson, Ariz.

Suess, H. E. (1955), Radiocarbon concentration in modern wood, *Science*, *122*, 415–417.

Therrell, M. D., D. W. Stahle, and M. K. Cleaveland (2002), Warm season tree growth and precipitation over Mexico, *J. Geophys. Res.*, *107*(D14), 4205, doi:10.1029/2001JD000851.

Treydte, K., et al. (2014), Seasonal transfer of oxygen isotopes from precipitation and soil to the tree ring: Source water versus needle water enrichment, *New Phytol.*, *202*(3), 772–783, doi:10.1111/nph.12741.

Vaganov, E. A., M. K. Hughes, and A. V. Shashkin (2006), *Growth Dynamics of Conifer Tree Rings*, *Ecol. Stud.*, Springer, Berlin.

Vaganov, E. A., E.-D. Schulze, M. V. Skomarkova, A. Knohl, W. A. Brand, and C. Roscher (2009), Intra-annual variability of anatomical structure and delta C-13 values within tree rings of spruce and pine in alpine, temperate and boreal Europe, *Oecologia*, *161*(4), 729–745, doi:10.1007/s00442-009-1421-y.

Vera, C., et al. (2006), Toward a unified view of the American monsoon systems, *J. Clim.*, *19*(20), 4977–5000, doi:10.1175/JCLI3896.1.

Wigley, T. M. L., K. R. Briffa, and P. D. Jones (1984), On the average value of correlated time series, with applications in dendroclimatology and hydrometeorology, *J. Clim. Appl. Meteorol.*, *23*(2), 201–213, doi:10.1175/1520-0450(1984)023<0201:OTAVOC>2.0.CO;2.

Williams, P. A., et al. (2013), Temperature as a potent driver of regional forest drought stress and tree mortality, *Nat. Clim. Change*, *3*(3), 292–297, doi:10.1038/nclimate1693.

Wright, W. E., A. Long, A. C. Comrie, S. W. Leavitt, T. Cavazos, and C. Eastoe (2001), Monsoonal moisture sources revealed using temperature, precipitation, and precipitation stable isotope timeseries, *Geophys. Res. Lett.*, *28*, 787–790, doi:10.1029/2000GL012094.